Epitaxial MOVPE growth of highly c-axis oriented InGaN/GaN films on ZnO-buffered Si (111) substrates

A. Ougazzaden[a], D. J. Rogers[b], F. Hosseini Teherani[b], G. Orsal[c], T. Moudakir[c], S. Gautier[c], V. E. Sandana[b], F. Jomard[d], M. Abid[a], M. Molinari[e], M. Troyon[e], P. L. Voss[a], D. McGrouther[f] & J. N. Chapman[f]

[a]Georgia Institute of Technology/GT-Lorraine-UMI 2958 Georgia Tech-CNRS, 2-3 rue Marconi, 57070 Metz, France
[b]Nanovation SARL, 103 bis Rue de Versailles, Orsay, 91400, France
[c]LMOPS - UMR CNRS 7132, Université de Metz et SUPELEC, 2 rue Edouard Belin, 57070 METZ, France
[d]GEMAC, Université de Versailles-Saint-Quentin1, place Aristide Briand, 92195 Meudon Cedex France
[e]LMEN, University of Reims Champagne-Ardennes, 21 rue Clement Ader, 51685 Reims, France
[f]Department of Physics and Astronomy, University of Glasgow, G12 8QQ, Scotland.

Corresponding author : aougazza@georgiatech-metz.fr

ABSTRACT

InGaN/GaN layers were grown on ZnO-buffered Si (111) substrates by metalorganic vapour phase epitaxy (MOVPE). The dissociation of ZnO observed during conventional MOVPE growth of InGaN/GaN was combated through the use of a low pressure/temperature MOVPE approach with N_2 as a carrier gas and dimethylhydrazine added to the ammonia (nitrogen precursor) in order to enhance the concentration of atomic nitrogen at relatively low temperature. Electron Microscopy of cross-sections, High Resolution X-Ray Diffraction (HR-XRD), secondary ion mass spectroscopy and cathodoluminescence studies suggested that single phase wurtzite InGaN layers with between about 17.5 and 21.5% indium were grown epitaxially, with no evidence of back-etching of the ZnO templates. HR-XRD revealed highly pronounced c-axis texture for both the InGaN/GaN and ZnO. Immersion in dilute nitric acid dissolved the ZnO such that the InGaN/GaN could be lifted-off from the substrate.

Keywords: metalorganic vapour phase epitaxy, InGaN, pulsed laser deposition, ZnO, Si substrate, lift-off

1. INTRODUCTION

Recently, the Gallium Nitride (GaN) and Zinc Oxide (ZnO) materials systems have attracted considerable attention because of their use in a broad range of emerging applications including light-emitting diodes [1-2] and solar cells [3-4]. GaN and ZnO are similar in that they have direct wide bandgaps, wurtzite crystal structure, high thermal stability and comparable thermal expansion coefficients. GaN has the advantage, however, of a mature know-how for p-type doping, while ZnO has proven to be more crystallographically compliant to non-native substrates than GaN. With a view to exploiting both of these strong points, ZnO layers have been proposed as buffer layers for the regrowth of GaN-based p-n devices on amorphous and mismatched substrates [5-9].

Alloying with In is important for engineering a reduced bandgap in GaN and thus facilitating quantum wells and devices which can function over the whole visible range. Previously, epitaxial growth of InGaN on ZnO has been reported on sapphire (Al_2O_3) substrates [10-11]. However, Al_2O_3 substrates are insulating, limited in size and relatively expensive. Silicon (Si) substrates, on the other hand, are cheaper, available in larger formats, have higher thermal/electrical conductivities and offer the potential for integration with mature Si-based electronics [12-13]. In this paper, we investigate the growth of InGaN/GaN on ZnO-buffered Si (111) substrates using metalorganic vapour phase epitaxy (MOVPE), which is the dominant growth technology for InGaN-based materials and devices.

One serious obstacle to the epitaxy of InGaN on ZnO is the stability of ZnO in the MOVPE process. In particular, exposure to ammonia (NH_3) precursor and H_2 carrier gas at growth temperatures over about 650°C results in the decomposition of the ZnO [14-15]. This can lead to the formation of interfacial layers/compounds, poor epitaxy and the unintentional incorporation of liberated Zn and O into the InGaN epilayer, which is detrimental for the optical and electrical properties.

2. EXPERIMENT

ZnO thin film templates were grown on 2-inch diameter Si (111) substrates using Pulsed Laser Deposition (PLD) with a Coherent KrF excimer laser (248nm) [5]. PLD was chosen because the high adatom mobility in this growth technique allows the ZnO to crystallise readily on amorphous substrates, such as the native SiO_2 passivation layer on the surface of the Si substrate. 40 nm thick GaN and InGaN layers (of various thicknesses) were then grown on the ZnO films using a low pressure, T-shaped, MOVPE reactor [16] with Trimethylgallium (TMG) as the Ga source and Trimethylindium (TMIn) as the In source. A combination of NH_3 and Dimethylhydrazine (DMHY) was used as a source of atomic nitrogen. DMHY was added because of its' low decomposition temperature, which enhances the concentration of atomic nitrogen in the gas phase compared to NH_3 alone, allowing GaN growth at lower temperatures. Nitrogen was employed as a carrier gas [17] during the whole growth process, in order to avoid etching of the ZnO surface and ensure In incorporation [18]. The impact of In content was studied by adjusting the TMIn flow at constant TMGa flow.

The surface roughness and growth rate of InGaN layers were monitored during the growth using in-situ reflectometry. Images of fracture cross-sectional samples were obtained using a Hitachi S-4800 field-emission scanning electron microscope (SEM). For transmission electron microscopy (TEM) investigation, cross-sectional samples were prepared using the in-situ liftout technique in a Dualbeam FIB (FEI Nova Nanolab 200). High resolution (HR-TEM) imaging was performed using an FEI Tecnai F20 equipped with a field emission gun source operated at 200 keV. The crystalline quality and indium composition of the InGaN layers were characterized by high resolution x-ray diffraction (HR-XRD), using Cu K_α radiation in Panalytical MRD-Pro system equipped with a hybrid monochromator.

Concentration profiles of In, Ga, N and Zn along the growth direction were obtained by MCs+ Secondary Ion Mass Spectroscopy (SIMS) in a Cameca IMS4F system. The primary (incident) ions were 133Cs+ with an impact energy of 5.5 keV. Positively charged secondary ions were detected. The optical properties of the InGaN/GaN/ZnO were studied using a home-made cathodoluminescence (CL) system in an SEM [19].

3. RESULTS & DISCUSSION

Figure 1 shows an SEM image of a fracture cross-section of an InGaN/GaN/ZnO/Si sample with approximately 21.5% In. The sample shows continuous InGaN/GaN and ZnO layers. A well-defined interface between ZnO and GaN can be clearly observed but the InGaN/GaN interface is not obvious. The thicknesses of the InGaN/GaN and ZnO are about 180nm and 140nm, respectively.
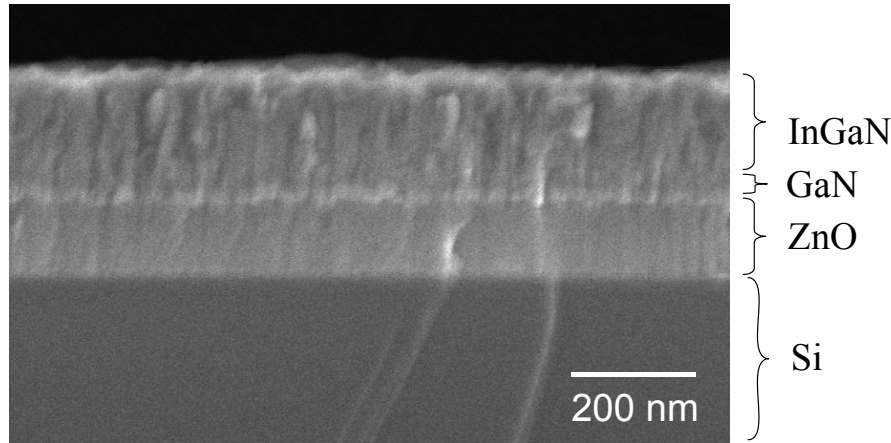

Figure 1. SEM fracture cross-section image of the InGaN/GaN/ZnO/Si heterostructure.

Figure 2 shows a HR-TEM image of the ZnO/Si interface. In this image, the regular lattice fringes in the Si substrate are interrupted at the interface with the ZnO due to the presence of the amorphous SiO_2 overlayer (~3nm thick). The subsequent ZnO layer shows established lattice fringes after only 2 nm of growth, confirming the capacity of PLD-grown ZnO to crystallise on amorphous substrates.
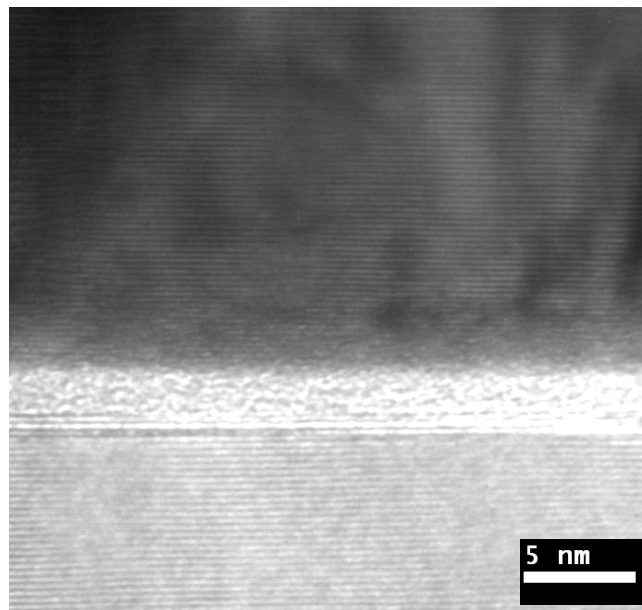

Figure 2. A HR-TEM image of the interface between the PLD-grown ZnO layer and the Si substrate.

Figure 3 shows a HR-TEM image of the interfaces between the InGaN, GaN and ZnO layers plus the result of a Fast Fourier Transform (FFT) analysis.
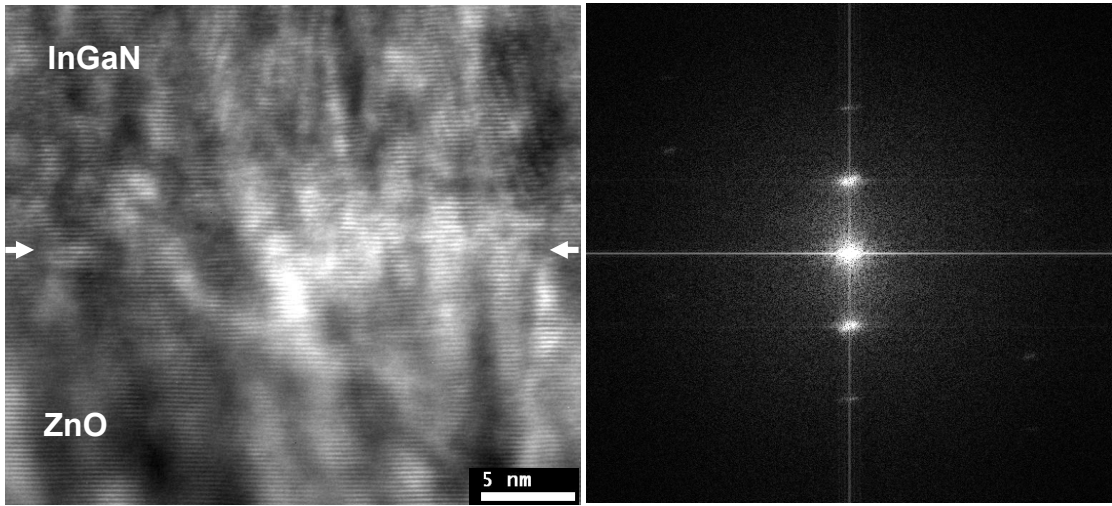

Figure 3. A HR-TEM image of the InGaN/GaN/ZnO interfaces plus a FFT analysis of the image (the arrows, in the former, suggest the position of GaN/ZnO interface).

The image shows continuous lattice fringes across the InGaN/GaN/ZnO interfaces, with no evidence of a misfit layer, or any interfacial compounds. The FFT confirms that both the lattice plane alignment and lattice spacing are similar in the InGaN/GaN and ZnO layers. Thus the TEM studies suggest that there has been epitaxial growth.

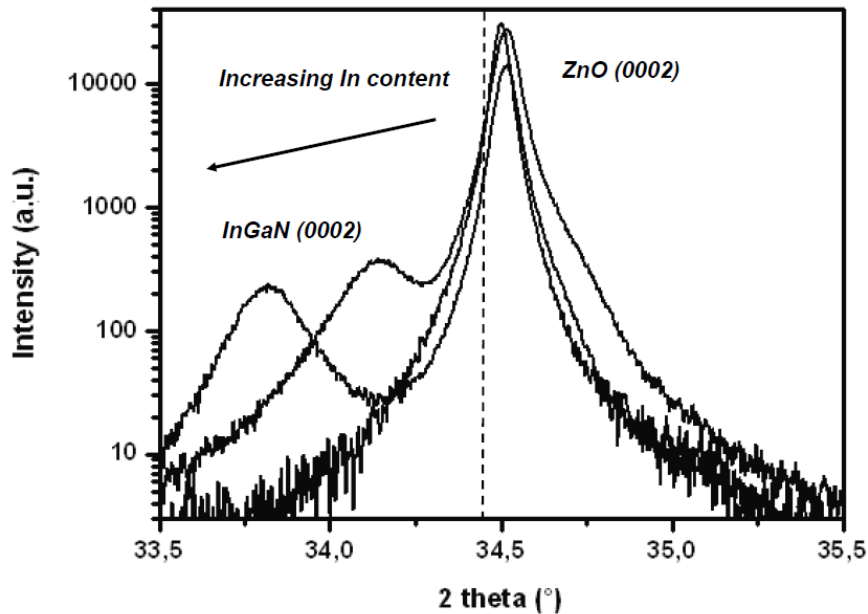Figure 4 shows the XRD 2θ-ω scans as a function of TMIn/III ratio during growth.

Figure 4. XRD 2θ-ω scans of the (0002) peak for ZnO/Si and the InGaN/GaN/ZnO/Si with varying In contents. The dashed line shows the peak position (34.43°) for a ZnO powder reference sample.

XRD study revealed the InGaN/GaN/ZnO layers to have single-phase wurtzite structure with strong c-axis orientation. The scans in Figure 4 present two distinct peaks, which were indexed as the (0002) peaks of the ZnO and the InGaN. An increase of the TMIn/III ratio led to a shift of the InGaN peak to lower angle and thus a higher out-of-plane "c" lattice parameter. The scans in Figure 4 also exhibited a small shoulder on the right of the ZnO peak, which was not visible in the XRD scans for the ZnO films prior to InGaN/GaN growth. This shoulder might be from the GaN layer. The concentration of In in the InGaN layer with higher In content (peak on left) was calculated from the (0002) InGaN peak position via Vegard's law to be about 21.5%. The (0002) ZnO peaks for all samples grown on Si were observed to be shifted to a higher 2θ angle than expected for bulk ZnO, which suggests that they were under tensile strain in the a-plane. This has been reported elsewhere for ZnO grown on Si substrates [20]. After InGaN/GaN growth, the ZnO peaks shifted slightly higher in 2θ (Figure 4). Thus the ZnO films absorbed some stress (tensile in this case) from the InGaN/GaN layers (as was observed in previous experiments on the MOVPE growth of GaN on ZnO/c-Al$_2$O$_3$ [6]).

Figure 5 shows the SIMS concentration profiles for Ga, In, N and Zn along the growth direction (in a sample with a thicker ZnO layer than that shown in Figure 1). The profile for Zn indicates some diffusion of Zn into the InGaN/GaN near the GaN/ZnO interface [8-9].
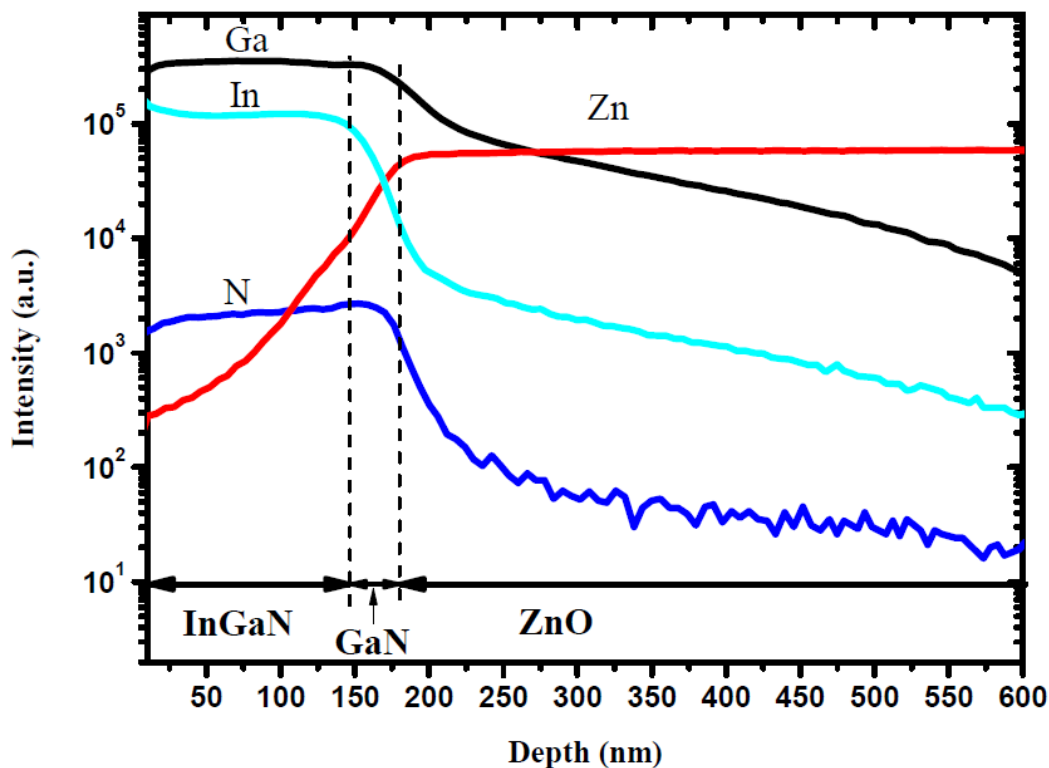

Figure 5. SIMS elemental concentration depth profiles for the Zn, Ga, N and In signals for the InGaN/GaN/ZnO-buffered Si (log. scale). It should be noted that the tails in the concentration profiles for In, Ga, and N, which extend into the ZnO, are probably artifacts due to residual particles of InGaN in the probe crater.

Figure 6 shows a normalized, room temperature (RT), CL spectrum plus a Monte Carlo simulation of the respective primary and back-scattered electron diffusion.
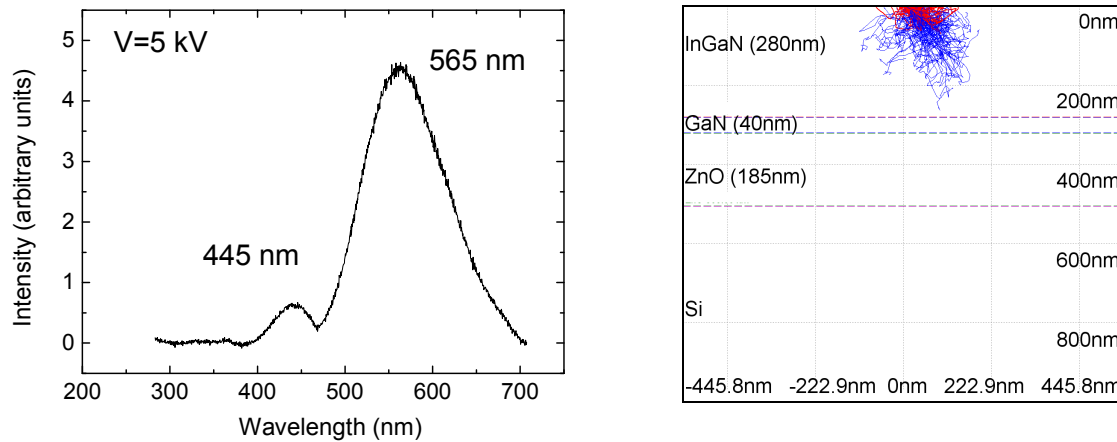

Figure 6. Normalized, RT, CL spectrum under 5kV accelerating voltage, plus a Monte Carlo simulation of the primary (red) and back-scattered (blue) electron diffusion.

The simulation suggested that an incident electron beam, with an energy of 5kV, stimulated a response from most of the InGaN/GaN layer depth. The spectrum itself shows two peaks located at about 445 nm (2.79 eV) and 565 nm (2.20 eV). The first of these peaks was indexed as InGaN with an In concentration of about 17.5 ± 5 % [21], which is coherent with the value calculated from the XRD scan. The second (565 nm) peak has been observed in InGaN grown on bulk ZnO in the past and has been attributed to emission from Zn-related impurity centers in the InGaN [22]. This is coherent with the slight diffusion of Zn into the InGaN/GaN near the interface with ZnO, which was observed by SIMS.
Finally, the InGaN/GaN was lifted-off the substrate by immersion in dilute HNO_3.
After several minutes, the ZnO dissolved completely and the InGaN/GaN separated from the substrate.

4. CONCLUSIONS

InGaN/GaN films were grown on ZnO-buffered Si (111) substrates by MOVPE. The dissociation of ZnO observed during conventional MOVPE growth of InGaN/GaN was combated through the use of a low pressure/temperature MOVPE approach with N_2 as a carrier gas and DMHY added to the NH_3 in order to facilitate atomic nitrogen production at lower temperatures. XRD, SEM, TEM, SIMS and CL characterisations showed smooth, highly c-axis oriented InGaN/GaN films having a well-defined interface with the ZnO underlayer, continuous lattice fringes across the interfaces and no evidence of any back-etching of ZnO. XRD and CL suggest that between 17.5 and 21.5% of In was integrated in the GaN, without any phase separation. Slight Zn diffusion into the InGaN/GaN was observed near the interface with ZnO.
Thus it was demonstrated that use of a PLD-grown ZnO buffer layer allows highly c-axis oriented wurtzite InGaN/GaN to be grown on Si substrates without removal of the amorphous SiO_2 layer. Such an approach may open the way to the integration of InGaN based devices with Si-based

electronics. The feasibility of chemical lift-off of the InGaN/GaN from the substrate was also demonstrated via dissolution of the ZnO in dilute HNO_3. Such a wet-etching approach would allow wafer bonding of the InGaN/GaN onto alternative substrates, with advantages such as superior transparency, and/or electrical/thermal conductivity.

ACKNOWLEDGEMENTS

REFERENCES

[1] X. Duan, Y. Huang, Y. Cui, J. Wang, C. M. Lieber, Nature 409 (2001) 66.
[2] T. Mukai, S. Nakamura, M. Senoh, Appl. Phys. Lett. 64 (1994) 1687.
[3] N. Golego, S. A. Studenkin, M. Cocivera, J. Electrochem. Soc. 147 (2000) 1592.
[4] S. C. Jain, M. Willander, J. Narayan, R. Van Overstraeten, J. Appl. Phys. 87 (2000) 965.
[5] D. J. Rogers, F. Hosseini Teherani, A. Yasan, R. McClintock, K. Mayes, S.R. Darvish, P. Kung, M. Razeghi, G. Garry, Proc. SPIE 5732 (2005) 412.
[6] D. J. Rogers, F. Hosseini Teherani, A. Ougazzaden, S. Gautier, L. Divay, A. Lusson, O. Durand, F. Wyczisk, G. Garry, T. Monteiro, M. R. Correira, M. Peres, A. Neves, D. McGrouther, J. N. Chapman, M. Razeghi, Appl. Phys. Lett. 91 (2007) 071120.
[7] A. Ougazzaden, D. J. Rogers, F. Hosseini Teherani, T. Moudakir, S. Gautier, T. Aggerstam S. Ould Saad, J. Martin, Z. Djebbour, L. Divay, O. Durand, G. Garry, A. Lusson, D. McGrouther, J. N. Chapman, J. Cryst. Growth 310 (2008) 944.
[8] D. J. Rogers, F. Hosseini Teherani, F. Jomard, M. Molinari, M. Troyon, D. McGrouther, J. N. Chapman, T. Moudakir, S. Gautier, A. Ougazzaden, M. Razeghi, J. Vac. Sci. Technol. B 273 (2009) 1655.
[9] R. Paszkiewicz, B. Paszkiewicz, M. Wosko, A. Szyszka, L. Marciniak, J. Prazmowska, W. Macherzynski, J. Serafinczuk, J. Kozowski, M. Tlaczala, J. Kovac, I. Novotny, J. Skriniarova, D. Hasko, J. Cryst. Growth 310 (2008) 4891.
[10] S.-J. Wang, N. Li, E.-H. Park, S.-C. Lien, Z. C. Feng, A. Valencia, J. Nause, I. Ferguson, J. Appl. Phys. 102 (2007) 106105.
[11] J.-B. Huang, S.-S. Wei, L.-C. Chen, L.-S. Hong, Solid-State Electronics (2008), doi:10.1016/j.sse.2008.03.007.
[12] M. Benyoucef, M. Kuball, B. Beaumont, P. Gibart, Appl. Phys. Lett. 81 (2002) 2370.
[13] J.W Lee, S.W Park, J.B. Yoo, Phys. Stat. Sol. A 176 (1999) 583.
[14] S.J. An, W.I. Park, G.C. Yi, Y.J. Kim, H.B. Kang, M. Kim, Appl. Phys. Lett. 84 (2004) 3612.
[15] K. Black, A.C. Jones, P.R. Chalker, J.M. Gaskell, R.T. Murray, T.B. Joyce, S.A. Rushworth, J. Crystal Growth 310 (2008) 1010.
[16] A. Mircea, A. Ougazzaden, R. Mellet, Prog. Cryst. Growth Charact. 19 (1989) 39.
[17] S. Gautier, C. Sartel, S. Ould-Saad, J. Martin, A. Sirenko, A. Ougazzaden, J. Cryst. Growth 298 (2007) 428.
[18] F. Scholz, V. Harle, F. Steuber, H. Bolay, A. Dornen, B. Kaufmann, V. Syganow, A. Hangleiter, J. Crystal Growth 170 (1997) 321.
[19] M. Troyon, D. Pastre, J. P. Jouart, and J. L. Beaudoin, Ultramicroscopy 75 (1998) 15.

[20] M. Suchea, S. Christoulakis, C. Tibeica, M. Katharakis, N. Kornilios, T. Efthimiopoulos, E. Koudoumas, Applied Surface Science, 254 (2008) 5475.

[21] S. Stepanov, W.N. Wang, B.S. Yavich, V. Bougrov, Y.T. Rebane, Y.G. Shreter, MRS Internet J. Nitride Semicond. Res. 6 (2001) 6.

[22] N. Li, S.-J. Wang, E.-H. Park, Z. C. Feng, A. Valencia, J. Nause, C. Summers, I. Ferguson, Proc. of SPIE Vol. 6669 (2007) 66690X-3.